The dynamics of a vesicle in shear flow

By H. Zhao AND E. S. G. Shaqfeh

1. Motivation

A vesicle is a viscous droplet enclosed by a lipid bilayer. The bilayer membrane behaves like a two-dimensional *incompressible* fluid in that it admits relative in-plane shear motion between lipid molecules without incurring any static shear stress. The membrane fluidity allows a clear distinction to be made between vesicles and capsules such as red blood cells, where the latter does have a reference shape because of the underlying spectrin network structure. The lipid bilayer nevertheless exhibits resistance to bending deformation because of the coupling between lipid layers. By assuming a homogeneous bilayer structure and zero spontaneous curvature, the simplest surface-bending energy functional model is (Evans 1974; Evans & Skalak 1980)

$$W_B = \frac{1}{2}\kappa \int_D (c_1 + c_2)^2 \, \mathrm{d}A, \tag{1.1}$$

where the integral is over the vesicle surface D, κ is the bending stiffness of the lipid bilayer, and $c_{1,2}$ are the two local principle curvatures.

We are interested in the rheology of vesicles in microfluidic devices, and have developed a simulation infrastructure using the boundary integral equation formulation that resolves the hydrodynamic interaction of vesicle–vesicle and vesicles–walls accurately and efficiently. Toward understanding the complex flow phenomena in microfluidic applications, we also simulate the simple system of a single vesicle in an unbounded shear flow of velocity field $u = \dot{\gamma} z$ where $\dot{\gamma}$ is the shear rate as shown in figure 1.

For a vesicle with constant volume V and constant surface area A, a measure of its aspherical shape without flow is given by the effective volume $v = 3V/(4\pi R^3)$ where $R = \sqrt{A/4\pi}$ is an effective vesicle length scale. All physical parameters can be non-dimensionalized by R, the bending stiffness κ, and the external fluid viscosity μ_{out}. The non-dimensional flow shear rate χ and the internal fluid viscosity are

$$\chi = \frac{\mu R^3 \dot{\gamma}}{\kappa} \qquad \text{and} \qquad \lambda = \frac{\mu_{\mathrm{in}}}{\mu_{\mathrm{out}}}. \tag{1.2}$$

The system is fully characterized by the three non-dimensional parameters: v, χ and λ. This is one of the simplest flow–structure interaction systems, and has been extensively studied experimentally (Kantsler & Steinberg 2005, 2006; Deschamps *et al.* 2009), theoretically (Keller & Skalak 1982; Seifert 1999; Hu *et al.* 2007; Lebedev *et al.* 2007; Noguchi & Gompper 2007; Vlahovska & Gracia 2007) and numerically (Kraus *et al.* 1996; Beaucourt *et al.* 2004; Meblinger *et al.* 2009). The agreement between experiments and small deformation theories is fairly poor when predicting the transition between different regimes of motion patterns (Deschamps *et al.* 2009; Lebedev *et al.* 2007). Although the recently discovered 'trembling' regime is also observed by simulations of the lattice Boltzmann type (Meblinger *et al.* 2009), it is difficult to make a clear distinction between different motion patterns because of the inherent thermal fluctuation in the simulation.

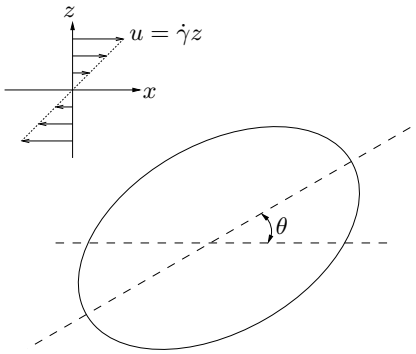

FIGURE 1. Schematics of a vesicle in a shear flow.

Our objective is to perform deterministic simulations by solving the governing Stokes flow equation and to compare the numerical results with theories and experiments.

The classic Keller–Skalak theory (Keller & Skalak 1982) predicts two flow regimes: a steady-state tank-treading motion where the vesicle assumes a steady-state ellipsoidal shape, and its inclination angle θ remains constant with time; the other is a tumbling regime where the vesicle rotates along the y-axis (the flow vorticity direction), and θ is periodic in time and varies in $[-\pi/2, \pi/2]$. The transition between the two regimes for a vesicle of fixed v happens at a critical viscosity ratio λ_c, beyond which the vesicle tumbles. Both tank treading and tumbling motions are observed in experiments (Kantsler & Steinberg 2005; Deschamps *et al.* 2009).

More recently a so-called 'trembling' regime has been reported (Kantsler & Steinberg 2006; Deschamps *et al.* 2009), where θ oscillates around 0 but its amplitude never reaches $\pi/2$. Similar trembling behavior is observed in numerical simulations using a multi-particle collision dynamics and is explained by a generalized Keller–Skalak theory (Noguchi & Gompper 2007; Meblinger *et al.* 2009). Here we simulate the vesicle in a shear flow using the Stokes flow boundary integral equations. Our formulation accurately captures the flow–structure interactions in a deterministic way while completely excluding thermal fluctuations.

2. Numerical methods

The surface velocity of a vesicle in an otherwise unperturbed shear flow $\mathbf{u}^0(\mathbf{x}) = (\chi z, 0, 0)$ is solved by a boundary integral formulation (Rallison & Acrivos 1978; Pozrikidis 1992),

$$\frac{1+\lambda}{2}\mathbf{u} - \frac{1-\lambda}{8\pi}\mathbf{K}\mathbf{u} + \frac{1}{8\pi\mu}\mathbf{N}[\![\mathbf{f}]\!] = \mathbf{u}^0, \tag{2.1}$$

where μ is the external flow viscosity and is unity by our non-dimensionalization, and $[\![\mathbf{f}]\!]$ is the total hydrodynamic force acting on the lipid bilayer. $\mathbf{N}$ and $\mathbf{K}$ are the single-layer and double-layer operators of the free space Stokes flow,

$$(\mathbf{N}\boldsymbol{\psi})_j(\mathbf{x}_0) = \int_D \psi_i(\mathbf{x}) G_{ij}(\mathbf{x}, \mathbf{x}_0)\, \mathrm{d}A(\mathbf{x}) \tag{2.2}$$

$$(\mathbf{K}\boldsymbol{\psi})_j(\mathbf{x}_0) = \int_D \psi_i(\mathbf{x}) T_{ijk}(\mathbf{x}, \mathbf{x}_0) n_k(\mathbf{x})\, \mathrm{d}A(\mathbf{x}), \tag{2.3}$$

where the Green's functions $\mathbf{G}$ (Stokeslet) and $\mathbf{T}$ (stresslet) are

$$G_{ij}(\mathbf{x},\mathbf{x}_0)=\frac{\delta_{ij}}{r}+\frac{\hat{x}_i\hat{x}_j}{r^3}\qquad T_{ijk}(\mathbf{x},\mathbf{x}_0)=-\frac{\hat{x}_i\hat{x}_j\hat{x}_k}{r^5} \tag{2.4}$$

with $\hat{\mathbf{x}}=\mathbf{x}-\mathbf{x}_0$ and $r=|\hat{\mathbf{x}}|$. The vesicle surface is discretized into a planar triangular mesh; standard piecewise linear boundary element and collocation methods are used to discretize equation (2.1) into a system of algebraic linear equations.

The surface force term $[\![\mathbf{f}]\!]$ consists of a bending force component $\mathbf{f}_B$ from membrane deformation and a constraint force $\mathbf{f}_\lambda$ due to surface incompressibility. The discrete bending energy W_B of the triangulated surface is calculated from the angles formed between neighboring elements (Boal & Rao 1992), and the bending force density is calculated by directly differentiating W_B with mesh deformation using the virtual work principle. For a mesh point α,

$$\mathbf{f}_B^\alpha\approx\frac{1}{A^\alpha}\frac{\partial W_B}{\partial\mathbf{x}^\alpha}, \tag{2.5}$$

where A^α is the surface area associated with point α that is calculated as one third of the total area of the triangles surrounding α. The discretized incompressibility condition of the surface velocity is

$$0=\frac{\mathrm{d}A^\alpha}{\mathrm{d}t}=\frac{\partial A^\alpha}{\partial\mathbf{x}^\beta}\cdot\mathbf{u}^\beta, \tag{2.6}$$

which introduces a Lagrange multiplier λ that is conjugate to vertex area (Kraus *et al.* 1996). The resulting constraint force density is

$$\mathbf{f}_\lambda^\alpha=\frac{1}{A^\alpha}\frac{\partial}{\partial\mathbf{x}^\alpha}\left(\sum_\beta\lambda^\beta A^\beta\right)=\frac{1}{A^\alpha}\sum_\beta\left(\lambda^\beta\frac{\partial A^\beta}{\partial\mathbf{x}^\alpha}\right)\qquad\text{(no sum over }\alpha\text{)}. \tag{2.7}$$

After splitting $[\![\mathbf{f}]\!]$ into $\mathbf{f}_B$ and $\mathbf{f}_\lambda$, equation (2.1) becomes

$$\left(\frac{1+\lambda}{2}\mathbf{I}-\frac{1-\lambda}{8\pi}\mathbf{K}\right)\mathbf{u}+\frac{1}{8\pi\mu}\mathbf{N}\mathbf{f}_\lambda=\mathbf{u}_0-\frac{1}{8\pi\mu}\mathbf{N}\mathbf{f}_B, \tag{2.8}$$

which must be solved jointly with equation (2.6).

The bending force density $\mathbf{f}_B=O(h^{-3})$ where h is mesh size; this stiffness makes it necessary to treat $\mathbf{f}_B$ implicitly if any reasonable time step size is to be used in time integration. We employ a linearized backward Euler scheme when solving (2.8),

$$\mathbf{f}_B^\alpha=\mathbf{f}_B^\alpha(t+\Delta t)\approx\mathbf{f}_B^\alpha(t)+\Delta t\mathbf{u}_\beta\cdot\frac{\partial\mathbf{f}_B^\alpha}{\partial\mathbf{x}^\beta}. \tag{2.9}$$

Since the vesicle does not have any reference shape, it is not necessary to treat mesh points as Lagrangian material points for surface evolution. Indeed, moving mesh points at the velocity $\mathbf{u}$ would always result in serious mesh distortion because of the in-plane shear. Instead, the mesh points are moved according to

$$\mathbf{x}(t+\Delta t)=\mathbf{x}(t)+\Delta t(u_\perp\mathbf{n}+\mathbf{u}_\parallel), \tag{2.10}$$

where $u_\perp=\mathbf{u}\cdot\mathbf{n}$ is the normal component of the physical velocity, and $\mathbf{u}_\parallel$ is on the local tangent plane. The latter is formulated to maintain a close-to-uniform mesh point distribution (Cristini *et al.* 2001). With the finite time step size in (2.10), the change to the surface shape is $O(\Delta t^2)$, which is consistent with the first-order time integration.

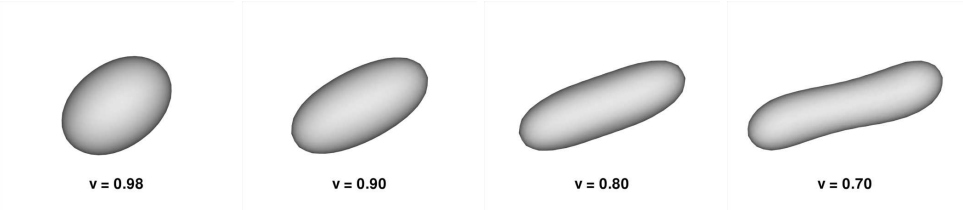

FIGURE 2. Shapes of steady-state tank-treading vesicles at $\lambda = 1$ and $\chi = 9$.

For very large surface deformations, the mesh quality can still deteriorate even with the aforementioned mesh relaxation. When the global minimum inner angle is below a threshold (here a 20° value is used), the mesh points are re-connected by a robust Delaunay triangulation (Si 2006).

3. Results

As a validation test, we simulate vesicles of matched internal and external viscosities ($\lambda = 1$) at shear rate $\chi = 9$, with the reduced volume $v \in (0.7, 0.98)$. The shapes of the steady-state tank-treading vesicles at four different v values are shown in figure 2. For nearly spherical vesicle (v close to 1), θ is close to $\pi/4$, as predicted by theory (Seifert 1999). The inclination angle decreases as v decreases, and the vesicle shape deviates from that of ellipsoids. At $v = 0.7$, the vesicle contour has become non-convex, thus maintaining the characteristic minimum energy shape in an quiescent flow. With increasing shear rate, a vesicle of any v value would eventually reach a ellipsoidal shape as the bending energy becomes negligible. In such extreme situations, the vesicle membrane merely serves as a geometrical constraint maintaining the conservation of surface area and the enclosed volume.

Figure 3 shows good agreement between the vesicle inclination angle θ obtained here and the simulation results by Kraus *et al.* (1996). In figure 4, the θ values are compared with the experimental results by Kantsler & Steinberg (2005), who also measured θ for mismatched viscosities at $\lambda = 2.7$ and 5.4. The agreement at $v \geq 0.9$ is remarkable for all three λ values; the decay of θ with v in our numerical results is slower than the power law fitted from the experimental data, but the differences are all within measurement uncertainties for $\lambda = 2.7$ and 5.4.

Tumbling motions are found at even higher values of internal viscosity. The time evolution of θ for a vesicle with $v = 0.9$ and $\lambda = 10$ is plotted in figure 5; the vesicle shapes at different stages of the tumbling cycling are shown in figure 6. Most noticeable is the continuous shape change during the tumbling cycle: the vesicle has an approximately prolate ellipsoidal shape at $\theta = 0$; the shape becomes non-axisymmetric and is blunted as the vesicle rotates counterclockwise till the longest axis is close to the z axis; after this point, the vesicle is elongated again and recovers its prolate ellipsoidal shape as θ approaches 0. The deformation can be described by the deformation parameter $D = (L - B)/(L + B)$, where L and B are the length of the long and short axes of the approximate ellipsoid in the x–z plane. The periodic variation of D is shown in figure 5.

Figure 7 shows the evolution of θ and D for a vesicle at $v = 0.85$, $\lambda = 6$ and $\chi = 20$. The inclination angle remains small, and the long axis never approaches z axis. During one motion cycle, θ first slowly decreases from 0 to a negative minimum, and then the vesicle shape undergoes a rapid change that flips the long and short axes so that θ reaches

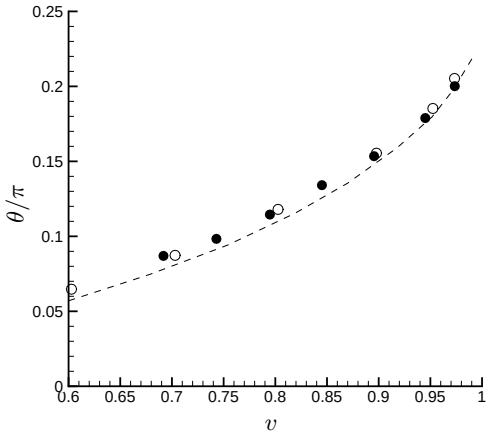

FIGURE 3. The inclination angle of steady-state tank-treading vesicles. The viscosity contrast $\lambda = 1$: ● is our simulation results at $\chi = 9$, ○ is by Kraus at $\chi = 10$ Kraus *et al.* (1996), and the dashed line is the theoretical prediction in Kraus *et al.* (1996).

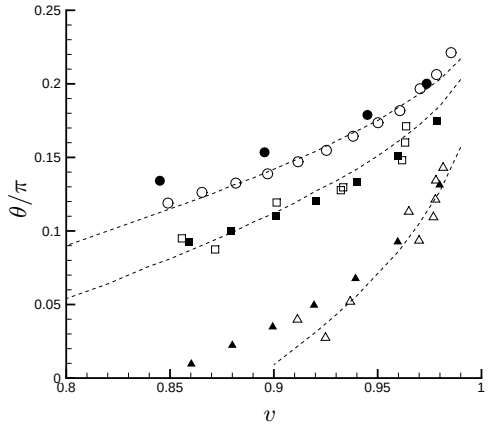

FIGURE 4. The inclination angle of vesicles at three different viscosity ratios: ● for $\lambda = 1$, ■ for $\lambda = 2.7$, and ▲ for $\lambda = 5.4$. The solid symbols are by our simulation; the empty symbols are from the experiment measurements of Kantsler & Steinberg (2005), and the dashed lines are the power law fitting of Kantsler.

a positive maximum shortly thereafter. Unlike the theoretical predictions by Noguchi & Gompper (2007), D remains over 0.2 during the whole period. Clearly this trembling pattern is caused by the competition between the deformation induced by the shear flow and the shape relaxation from the membrane bending stiffness and warrants further study.

4. Future plan

The three patterns of vesicle motion—tank-treading, tumbling and trembling—are all observed unambiguously in our deterministic simulations. Currently, the three-dimensional parametric space (v, λ, and χ) is being scanned. Unlike the Keller–Skalak theory where χ

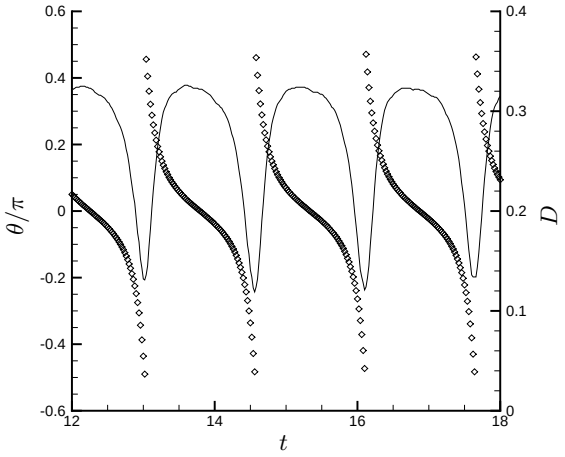

FIGURE 5. Inclination angle θ and deformation parameter D of a tumbling vesicle: $\diamond$ is for θ and ——— is for D. The simulation is at $v = 0.9$, $\lambda = 10$ and $\chi = 8$.

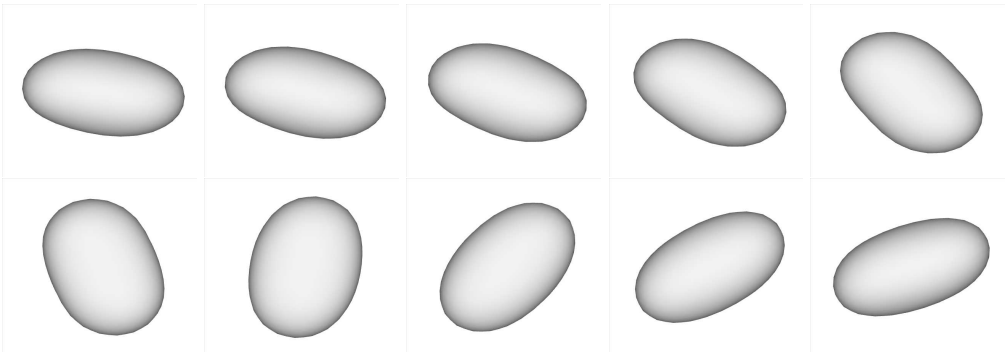

FIGURE 6. The shape of a vesicle during a tumbling cycle. The parameters are the same as those in figure 5. Any two subsequent snapshots are separated by a 0.1 time interval.

is merely a scaling factor, shear rate indeed is an important parameter for the transition between different regimes. We also plan to study the time evolution of spherical harmonic modes of vesicle shape, which should give a clear picture of the underlying mechanism during the rapid flip of θ in the trembling regime.

REFERENCES

BEAUCOURT, J., RIOUAL, F., SEON, T., BIBEN, T. & MISBAH, C. 2004 Steady to unsteady dynamics of a vesicle in a flow. *Phys. Rev. E* **69**, 011906.

BOAL, D. H. & RAO, M. 1992 Topology changes in fluid membranes. *Phys. Rev. A* **46** (6), 3037.

CRISTINI, V., BLAWZDZIEWICZ, J. & LOEWENBERG, M. 2001 An adpative mesh algrithm for evolving surfaces: simulation of drop break up and coalescence. *J. Comput. Phys.* **168** (2), 445–463.

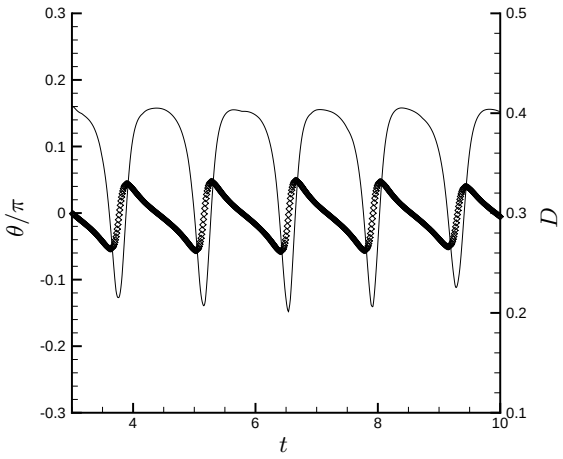

FIGURE 7. Inclination angle θ and deformation parameter D of a seemingly trembling vesicle: $\diamond$ is for θ and ——— is for D. The simulation is at $v = 0.85$, $\lambda = 6$ and $\chi = 20$.

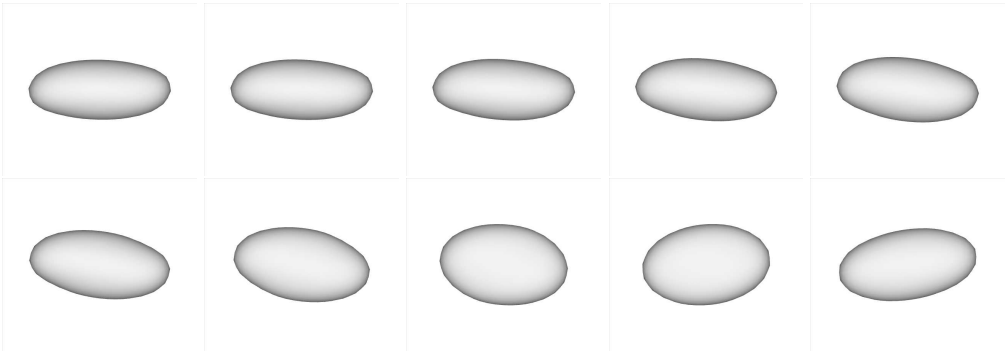

FIGURE 8. The shape of a vesicle during a trembling cycle. The parameters are from the same simulation plotted in figure 7. Any two subsequent snapshot is separated by 0.1 time interval.

DESCHAMPS, J., KANTSLER, V. & STEINBERG, V. 2009 Phase diagram of single vesicle dynamical states in shear flow. *Phys. Rev. Lett.* **102**, 118105.

EVANS, E. A. 1974 Bending resistance and chemically induced moments in membrane bilayers. *Biophs. J.* **14**, 923–931.

EVANS, E. A. & SKALAK, R. 1980 *Mechanics and Thermodynamics of Biomembranes*. CRC.

HU, D., ZHANG, P. & E, W. 2007 Continuum theory of a movin membrane. *Phys. Rev. E* **75**, 041605.

KANTSLER, V. & STEINBERG, V. 2005 Orientation and dynamics of a vesicle in tank-treading motion in shear flow. *Phys. Rev. Lett.* **95**, 258101.

KANTSLER, V. & STEINBERG, V. 2006 Transition to tumbling and two regimes of tumbling motiion of a vesicle in shear flow. *Phys. Rev. Lett.* **96**, 036001.

KELLER, S. R. & SKALAK, R. 1982 Motion of a tank-treading ellipsoidal particle in a shear flow. *J. Fluid Mech.* **120**, 27–47.

Kraus, M., Wintz, W., Seifert, U. & Lipowsky, R. 1996 Fluid vesicles in shear flow. *Phys. Rev. Lett.* **77** (17), 3685–3688.

Lebedev, V. V., Turitsyn, K. S. & Vergeles, S. S. 2007 Dynamics of nearly spherical vesicles in an external flow. *Phys. Rev. Lett.* **99**, 218101.

Meblinger, S., Schmidt, B., Noguchi, H. & Gompper, G. 2009 Dynamical regimes and hydrodynamic lift of viscous vesicles under shear. *Phys. Rev. E* **80**, 011901.

Noguchi, H. & Gompper, G. 2007 Swinging and tumbling of fluid vesicles in shear flow. *Phys. Rev. Lett.* **98**, 128103.

Pozrikidis, C. 1992 *Boundary Integral and Singularity Methods for Linearized Viscous Flow*. Cambridge: Cambridge University Press.

Rallison, J. M. & Acrivos, A. 1978 A numerical study of the deformation and burst of a viscous drop in an extensional flow. *J. Fluid Mech.* **89**, 191–200.

Seifert, U. 1999 Fluid membranes in hdrodynamic flow fields: Formalism and an application to fluctuating quasispherical vesicles in shear flow. *Eur. Phys. J. B* **8**, 405–415.

Si, H. 2006 TetGen: A quality tetrahedral mesh generator and three-dimensional Delaunay triangulatior.

Vlahovska, P. M. & Gracia, R. S. 2007 Dynamics of a viscous vesicle in linear flows. *Phys. Rev. E* **75**, 016313.